THE JOURNAL OF BIOLOGICAL CHEMISTRY VOL. 289, NO. 14, pp. 9865–9879, April 4, 2014

Human Immunodeficiency Virus Type 1 Enhancer-binding Protein 3 Is Essential for the Expression of Asparagine-linked Glycosylation 2 in the Regulation of Osteoblast and Chondrocyte Differentiation*[S]

Received for publication, September 20, 2013, and in revised form, January 26, 2014 Published, JBC Papers in Press, February 21, 2014, DOI 10.1074/jbc.M113.520585

Katsuyuki Imamura[‡§], Shingo Maeda[‡1], Ichiro Kawamura[§], Kanehiro Matsuyama[‡§], Naohiro Shinohara[‡§], Yuhei Yahiro[‡§], Satoshi Nagano[§], Takao Setoguchi[¶], Masahiro Yokouchi[§], Yasuhiro Ishidou[‡], and Setsuro Komiya[‡§¶]

From the Departments of [‡]Medical Joint Materials and [§]Orthopaedic Surgery and the [¶]Near-Future Locomotor Organ Medicine Creation Course, Graduate School of Medical and Dental Sciences, Kagoshima University, Kagoshima 890-8544, Japan

Background: The mechanisms by which Hivep3 regulates the osteochondrogenesis remain elusive.
Results: Knockdown of Hivep3 down-regulated *Alg2* expression. Alg2 suppressed osteoblast differentiation by inhibiting the activity of Runx2. Alg2 silencing suppressed the expression of *Creb3l2* and chondrogenesis.
Conclusion: Alg2 may be a modulator of osteochondrogenesis.
Significance: This is the first report to describe the association of an Alg gene with osteochondrogenesis.

Human immunodeficiency virus type 1 enhancer-binding protein 3 (*Hivep3*) suppresses osteoblast differentiation by inducing proteasomal degradation of the osteogenesis master regulator Runx2. In this study, we tested the possibility of cooperation of Hivep1, Hivep2, and Hivep3 in osteoblast and/or chondrocyte differentiation. Microarray analyses with ST-2 bone stroma cells demonstrated that expression of any known osteochondrogenesis-related genes was not commonly affected by the three Hivep siRNAs. Only *Hivep3* siRNA promoted osteoblast differentiation in ST-2 cells, whereas all three siRNAs cooperatively suppressed differentiation in ATDC5 chondrocytes. We further used microarray analysis to identify genes commonly down-regulated in both MC3T3-E1 osteoblasts and ST-2 cells upon knockdown of *Hivep3* and identified asparagine-linked glycosylation 2 (*Alg2*), which encodes a mannosyltransferase residing on the endoplasmic reticulum. The *Hivep3* siRNA-mediated promotion of osteoblast differentiation was negated by forced Alg2 expression. Alg2 suppressed osteoblast differentiation and bone formation in cultured calvarial bone. Alg2 was immunoprecipitated with Runx2, whereas the combined transfection of Runx2 and Alg2 interfered with Runx2 nuclear localization, which resulted in suppression of Runx2 activity. Chondrocyte differentiation was promoted by Hivep3 overexpression, in concert with increased expression of *Creb3l2*, whose gene product is the endoplasmic reticulum stress transducer crucial for chondrogenesis. *Alg2* silencing suppressed *Creb3l2* expression and chondrogenesis of ATDC5 cells, whereas infection of Alg2-expressing virus promoted chondrocyte maturation in cultured cartilage rudiments. Thus, Alg2, as a downstream mediator of Hivep3, suppresses osteogenesis, whereas it promotes chondrogenesis. To our knowledge, this study is the first to link a mannosyltransferase gene to osteochondrogenesis.

In skeletal development and bone remodeling, osteoblasts play major roles not only in bone formation but also in inducing the differentiation of bone-resorbing osteoclasts (1, 2). Runx2 is a critical transcription factor in osteoblast differentiation, as evidenced by Runx2 knock-out mice, which exhibit a complete lack of both intramembranous and endochondral ossification due to the absence of osteoblasts (3). Cleidocranial dysplasia, a human autosomal dominant inherited disorder of bone development, is characterized by hypoplasia of clavicles and abnormalities in cranial and facial bones and is caused by mutations in the *Runx2* gene (4, 5). Some genes, *e.g.* LDL receptor-related protein 5 (*Lrp5*), sclerostin (*Sost*), and human immunodeficiency virus type 1 enhancer-binding protein 3 (*Hivep3*), have been found to control osteoblast function in the adult human and/or mouse during postnatal skeletal remodeling (6–10).

Hivep3, also known as Schnurri-3, Zas3, and Krc, is a member of three mammalian homologs of the Hivep/Schnurri family of large zinc finger proteins. Hivep proteins have been studied for their roles in the regulation of an assortment of genes, including those encoding collagen type IIA, αA-crystallin, β-interferon, and HIV genes (11). Hivep2 can indirectly interact with the peroxisome proliferator-activated receptor γ2 (*Pparg2*) promoter to promote adipogenesis, through binding to Smad1, an intracellular mediator of bone morphogenetic protein (BMP)[2] signaling. Hivep2 can also dock to CCAAT/enhancer-binding protein α (C/ebpα) to interact

* This work was supported by Japan Society for the Promotion of Science KAKENHI Grants 23592221 (to S. M.) and 23592222 (to Y. I.), a grant from the Cell Science Research Foundation (to S. M.), and a grant from the Hip Joint Foundation of Japan (to S. M.).
[S] This article contains supplemental Tables 1–5.
[1] To whom correspondence should be addressed: Dept. of Medical Joint Materials, Graduate School of Medical and Dental Sciences, Kagoshima University, 8-35-1 Sakuragaoka, Kagoshima 890-8544, Japan. Tel.: 81-99-275-5381; Fax: 81-99-265-4699; E-mail: maeda-s@umin.ac.jp or s-maeda@m3.kufm.kagoshima-u.ac.jp.

[2] The abbreviations used are: BMP, bone morphogenetic protein; ER, endoplasmic reticulum; ALP, alkaline phosphatase; ECM, extracellular matrix; CDG, congenital disorders of glycosylation; qRT, quantitative RT; ALG, asparagine-linked glycosylation.

with a CCAAT site on the distal part of the *Pparg* gene (12). Mice lacking Hivep3 demonstrate adult-onset osteosclerosis with increased bone volume due to enhanced osteoblast activity (10). Hivep3 promotes proteasomal degradation of the Runx2 protein through recruitment of the E3 ubiquitin ligase Wwp1 to Runx2 (10). A D-domain motif within Hivep3 mediates the interaction with and inhibition of ERK mitogen-activated protein kinase (MAPK), thereby inhibiting Wnt/Lrp5 signaling through regulation of the activity of a downstream mediator glycogen synthase kinase 3-β (Gsk3β). This interaction results in the suppression of subsequent osteoblast differentiation (13). In addition, Hivep3 indirectly promotes osteoclastogenesis by promoting osteoblastic expression of receptor activator of nuclear factor-κB ligand (Rankl), a crucial factor for osteoclast differentiation (14). Hivep3 also cell-autonomously promotes osteoclastogenesis by inducing the expression of *Nfatc1*, a master transcription factor in osteoclast differentiation, by interacting with Traf6 to enhance its activity while forming a complex with c-Jun to activate the *Nfatc1* promoter (15). Thus, Hivep3 controls both bone formation and resorption at multiple steps to maintain normal bone mass. However, whether Hivep3 controls gene expression in osteoblasts to regulate osteoblast activity is unclear.

In contrast to *Hivep3* knock-out mice, mice lacking *Hivep2* exhibited decreased cortical bone volume and increased cancellous bone mass (16), suggesting different roles for Hivep2 and Hivep3 in the skeleton. Combined ablation of *Hivep2* and *Hivep3* in mice resulted in synergistically increased trabecular bone volume, demonstrating a redundancy between the two proteins in the regulation of postnatal bone mass (17). Interestingly, in the double knock-out mice, the growth plate cartilage of the long bones was uncoupled with bone phenotype, with significantly delayed maturation of chondrocytes resulting in chondrodysplasia (17), suggesting a role for Hivep proteins in the promotion of chondrocyte differentiation. However, the mechanism by which Hivep proteins affect chondrogenesis remains unknown. In addition, to date, no information has been reported on the possible role of Hivep1 in osteogenesis and/or chondrogenesis.

In this study, *in vitro* analysis showed that, among the three Hivep proteins, only Hivep3 was inhibitory and that the others promoted osteoblast differentiation. In contrast, all three Hivep genes seemed to support chondrocyte differentiation in BMP-2-induced ATDC5 cells, suggesting their redundancy in chondrogenesis. We found that asparagine-linked glycosylation 2 (*Alg2*) is commonly down-regulated in BMP-2-induced osteoblast differentiation in both MC3T3-E1 and ST-2 cells. Alg2 inhibited Runx2 activity without altering its protein level, resulting in suppression of osteoblast differentiation. Interestingly, in chondrogenesis of ATDC5 cells, Hivep3 induced the expression of cAMP-responsive element binding-protein 3-like 2 (*Creb3l2*), an endoplasmic reticulum (ER) stress transducer crucial for chondrogenesis (18), suggesting a possible role for Hivep3 in physiological mild ER stress. Alg2 was also decreased by *Hivep3* knockdown in ATDC5 chondrocytes, whereas silencing of Alg2 suppressed the expression of *Creb3l2* and chondrogenesis. To our knowledge, this study is the first to show a linkage between an asparagine-linked glycosylation mannosyltransferase gene and osteochondrogenesis.

EXPERIMENTAL PROCEDURES

Cell Culture and Differentiation—The mouse calvarial bone-derived osteoblast cell line, MC3T3-E1 (clone 4), and the mouse chondrogenic fibroblast cell line, C3H10T1/2, were obtained from the ATCC. The mouse bone marrow stromal cell line ST-2 and the mouse chondrogenic cell line ATDC5 were obtained from the RIKEN BioResource Center. MC3T3-E1 cells were cultured in minimum essential medium α (Invitrogen) containing 10% fetal bovine serum (FBS). ST-2 cells were cultured in RPMI 1640 medium (Sigma) containing 10% FBS. ATDC5 cells were cultured in Dulbecco's modified Eagle's medium (DMEM)/Ham's F-12 (1:1) (Invitrogen) containing 5% FBS. C3H10T1/2 cells were cultured in basal medium Eagle's (Sigma) with 2 mM L-glutamine and 10% FBS. COS-7 cells were purchased from RIKEN BioResource Center and maintained in DMEM supplemented with 10% FBS. All cell culture medium contained 100 units/ml penicillin G and 100 μg/ml streptomycin. Cell differentiation was induced by the addition of recombinant human BMP-2 (PeproTech) at a concentration of 300 ng/ml. Micromass culture of ATDC5 cells was performed as described previously (19) to accelerate the maturation of chondrocyte differentiation.

Alkaline Phosphatase (ALP) and Alcian Blue Staining—The activity of ALP secreted into the extracellular matrix (ECM) of cultured cells was visualized with an ALP staining kit (85L-3R, Sigma). Cartilaginous glycosaminoglycans produced in the ECM by cultured cells were stained with Alcian blue 8GX (Sigma).

RNA Interference—Dharmacon siRNA ON-TARGETplus SMARTpool, a mixture of four independent siRNAs against mouse *Hivep1*, *Hivep2*, *Hivep3*, and *Alg2*, and the control reagent were purchased from Thermo Scientific. siRNAs were transfected into cells using Lipofectamine RNAiMax (Invitrogen).

Real Time Quantitative PCR—Cells were lysed with TRIzol reagent (Invitrogen) to purify RNA, and 1 μg of total RNA was subjected to reverse transcription with the Verso cDNA kit (Thermo Scientific). The relative amounts of the gene transcripts were determined by real time quantitative PCR using SYBR premix Ex TaqII (Takara) and the Thermal Cycler Dice TP850 system (Takara). PCRs were performed in duplicate per sample, and the measured expression level of each gene was normalized to that of *Hprt1*. The sequence information for the primers used is listed in supplemental Table 1. All primer sets are for mouse genes, except for the m/h*Hivep3* primer set, which can be used to amplify both the mouse and human *Hivep3* genes. For evaluation of the tissue distribution of the Hivep genes and Alg2 *in vivo*, tissues were harvested from 3-month-old mice, and mRNA was purified with TRIzol reagent before subjecting samples to qRT-PCR.

Microarray Analysis—Cells transfected with siRNA overnight were further incubated with BMP-2 for 2 days before being lysed with TRIzol reagent for mRNA purification. mRNA samples were cleaned up using the RNeasy MinElute Cleanup kit (Qiagen) and analyzed on a Mouse Gene 2.0 ST Array (Affymetrix) by BioMatrix Research.

Plasmids, Adenovirus, and Lentivirus—The mouse Hivep3 expression plasmid, pEF-Shn3, was a kind gift from Dr. Laurie Glimcher (Harvard Medical School). The human HIVEP3 expression plasmid pFN21A-HIVEP3 was obtained from Kazusa DNA Research Institute. The mouse type II Runx2 expression plasmid was a kind gift from Dr. Toshihisa Komori (Nagasaki University). The FLAG-Runx2-def expression plasmid has been described in our previous study (20). Mouse *Alg2* or *Runx2* cDNA was cloned from ST-2 cells by using a RT-PCR-based technique, subcloned into the entry vector, pENTR, and further transferred into the C-terminally V5-tagged expression vector, pEF-DEST51 (Invitrogen). For overexpression assays, cells were transfected with expression vectors using FuGENE 6 (Roche Applied Science) or Lipofectamine 2000 (Invitrogen). Cells transiently expressing the transgenes were selected and enriched by incubation with G418 disulfate (Nacalai Tesque) at a concentration of 250 μg/ml for 3–7 days. To generate adenovirus-carrying *Alg2* cDNA, the *Alg2* gene in the pENTR-Alg2 vector was transferred into the C-terminally V5-tagged adenovirus expression vector pAd/CMV/V5-DEST by LR recombination (Invitrogen) and was further transfected into the adenovirus-producing cell line 293A according to the manufacturer's protocol. The pAd/CMV/V5-GW/lacZ adenovirus expression vector was used to generate a control adenovirus. For generation of lentivirus carrying the *Alg2* gene, pENTR-Alg2 and pENTR-5′EF1αP were subjected to LR recombination with pLenti6.4/R4R2/V5-DEST (Invitrogen) to generate a lentiviral vector expressing C-terminally V5-tagged Alg2 from the EF1α promoter. The lentiviral expression vector or pLenti6/V5/GW-lacZ control vector was transfected into 293FT cells to generate the lentivirus. Virus infection into ST-2 cells was performed at a multiplicity of infection of 100. Cells infected with the lentivirus were selected by treatment with blasticidin S HCl (Invitrogen) at a concentration of 2.5 μg/ml. These experiments were approved by the Kagoshima University safety control committee for gene recombination techniques (number 22053).

Embryonic Bone Organ Culture—Calvarial bone and metatarsal bone (cartilage) rudiments were harvested from C57BL/6J mouse embryos at 17.5 days post-coitum (E17.5) and cultured in minimum essential medium α or DMEM/Ham's F-12 (1:1), respectively, supplemented with 10% FBS, 100 units/ml penicillin G, and 100 μg/ml streptomycin, as described (21). The bone rudiments were incubated in virus solution overnight for infection of adenovirus or lentivirus. Cultured bones and cartilages were fixed in 96% ethanol and stained with 0.015% Alcian blue 8GX in a mixture solution of 96% ethanol/acetic acid (4:1) for 1 day, followed by a dehydration step in 100% ethanol. Dehydrated bones were immersed briefly in 1% potassium hydroxide (KOH), followed by staining in 0.001% alizarin red S (Sigma) in 1% KOH for 1 day. Images were captured with stereomicroscope M165FC (Leica). The animal experiments were approved by the Institutional Animal Care and Use Committee of Kagoshima University (number MD12137).

Immunoprecipitation and Immunoblotting—For immunoprecipitation assays, COS-7 cells were transfected with Alg2-V5 and/or FLAG-Runx2 plasmids and were lysed in M-PER lysis buffer (Thermo Scientific) supplemented with aprotinin and phenylmethylsulfonyl fluoride (PMSF). The lysate was immunoprecipitated with anti-FLAG M2-agarose affinity gel (A2220, Sigma), and the M2 antibody-bound protein complex was eluted by incubation with 3×FLAG peptide (F4799, Sigma), according to the manufacturer's protocol. For immunoblotting assays, cells were lysed in either M-PER or NE-PER lysis buffer (Thermo Scientific) supplemented with aprotinin and PMSF or directly with 1× SDS sample buffer. SDS-PAGE, membrane transfer, and chemiluminescence were performed using a standard protocol. The blots were incubated with primary antibodies against Alg2 (1:1000; LS-C81338, Lifespan Biosciences), Runx2 (1:200; M-70, sc-10758, Santa Cruz Biotechnology), Runx2 (1:1000; 8G5, MBL), Sp7 (1:1000, ab22552, Abcam), Ibsp (1:1000, LS-C190916, Lifespan Biosciences), type II collagen (1:1000, LS-C175971, Lifespan Biosciences), Creb3l2 (1:1000, ab76856, Abcam), V5 (1:5000; R960-25, Invitrogen), FLAG (1:1000; M2, F1804, Sigma), and tubulin (1:1000; DM1A, T9026, Sigma) and with horseradish peroxidase (HRP)-conjugated anti-rabbit and anti-mouse secondary antibodies (1:10,000) (Cell Signaling). For examination of half-life of Runx2 protein, after overnight transfection with siRNA of *Hivep3*, ST-2 cells were treated with cycloheximide (Sigma) at 100 μg/ml, followed by immunoblotting using anti-Runx2 antibody. Signals were detected using the LAS 4000 mini image analyzer (Fujifilm).

Immunofluorescence—For immunofluorescence assays, cells transfected with Runx2 and/or Alg2-V5 expression plasmids were fixed with 4% paraformaldehyde in PBS for 30 min and treated with 0.2% Triton X-100. CAS block (Zymed Laboratories Inc.) was used for blocking. Cells were incubated with anti-Runx2 (1:100; 8G5, MBL), Alexa Fluor 568 rabbit anti-mouse IgG (1:1000; A11061, Invitrogen), and anti-V5-FITC (1:500; R619-25, Invitrogen) antibodies. Nuclei were stained with Hoechst dye (Invitrogen). Confocal fluorescent imaging was performed and analyzed using a laser scanning microscope system (LSM 700, Zeiss). For confirmation of the efficiency of virus infection in cultured bones, formalin-fixed mouse E17.5 embryo calvariae or metatarsal bones were embedded in paraffin blocks, which were sliced at a 4-μm thickness. The antigen was retrieved by Liberate Antibody Binding (L.A.B.) solution (Polysciences). A CAS block was used for blocking. Bone sections were incubated with anti-V5-FITC antibody. Images were captured with microscope AX80 and digital camera DP70 (Olympus).

Luciferase Assay—COS-7 cells or ST-2 cells were seeded in triplicate in 24-well plates and transiently transfected with the 6×OSE2 luciferase reporter plasmid (a kind gift from Dr. Toshihisa Komori), the mutant 6×OSE2 luciferase reporter plasmid (a kind gift from Dr. Gerard Karsenty, Columbia University Medical Center), the pGL4.75hRlucCMV *Renilla* vector (Promega), and expression vectors for Runx2, Alg2, or Hivep3. Dual-Luciferase assays were performed as described earlier (20) by using the GloMax 96 microplate luminometer (Promega).

Statistical Analysis—The data in this study have been expressed as mean ± S.D. values of three independent experiments. Statistical comparisons between the different treatments were performed using an unpaired Student's *t* test in

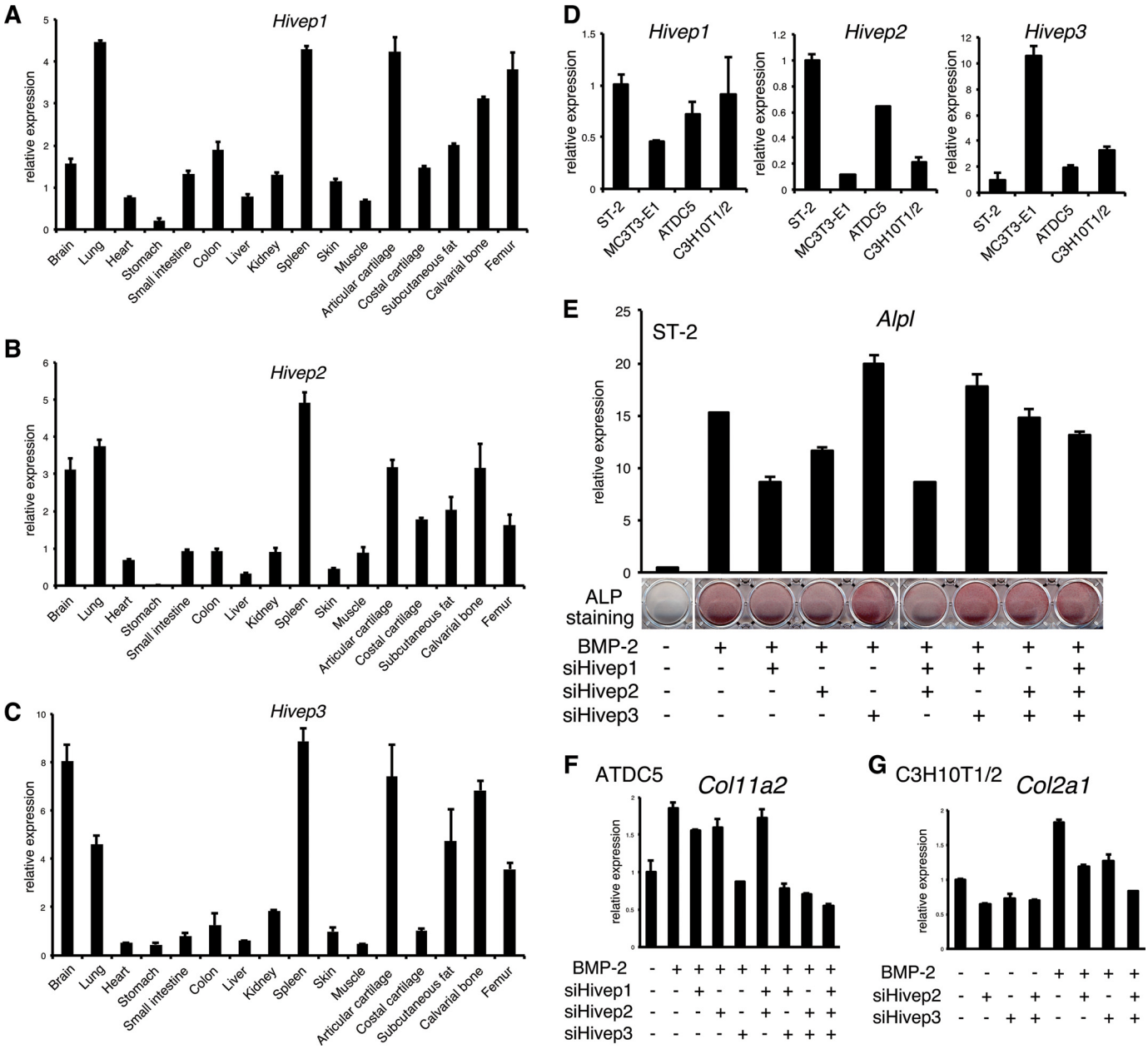

FIGURE 1. **All three Hivep genes are expressed in bone and cartilage to support osteochondrogenesis except Hivep3, which is inhibitory for osteoblast differentiation.** *A–C*, tissue cDNA panel of a 3-month-old mouse was subjected to quantitative RT-PCR (qRT-PCR) for *Hivep1* (*A*), *Hivep2* (*B*), or *Hivep3* (*C*). *D*, expression level of *Hivep1*, *Hivep2*, or *Hivep3* in the indicated cell lines was examined by qRT-PCR. *E*, ST-2 cells were transfected with siRNA for *Hivep1*, *Hivep2*, or *Hivep3* and treated with BMP-2 (300 ng/ml) for 6 days. Expression of *Alpl* was analyzed by qRT-PCR, and activity of ALP on ECM was visualized by ALP staining. *F*, ATDC5 cells were transfected with siRNA for *Hivep1*, *Hivep2*, and/or *Hivep3* and treated with BMP-2 (300 ng/ml) for 3 days. Expression of *Col11a2* was evaluated by qRT-PCR. *G*, C3H10T1/2 cells were transfected with siRNA for *Hivep2* and/or *Hivep3* and treated with BMP-2 (300 ng/ml) for 4 days. Expression of *Col2a1* was analyzed by qRT-PCR.

which $p < 0.05$ was considered significant, and $p < 0.01$ was considered highly significant.

RESULTS

Loss of Hivep1 or Hivep2 Suppresses Osteoblast Differentiation in ST-2 Cells, in Contrast to Hivep3 Silencing, and All Three Hivep siRNAs Inhibited Chondrogenesis—The precise roles of Hivep1 and Hivep2 in osteoblast differentiation are unclear. In a tissue cDNA panel from a 3-month-old adult mouse, all the Hivep genes showed a relatively specific expression pattern with high expression being observed in the lung, spleen, articular cartilage, and bone (Fig. 1, *A–C*). However, the *in vitro* results for the osteochondrogenic cell lines ST-2, MC3T3-E1, ATDC5, and C3H10T1/2 showed that the expression profiles were completely different between the Hivep genes, with *Hivep1* being expressed ubiquitously, *Hivep2* abundant in ST-2 and ATDC5, and *Hivep3* prominent in MC3T3-E1 osteoblasts (Fig. 1*D*). If the Hivep genes cooperate in osteoblast differentiation, they should regulate some common sets of genes. To test this hypothesis, ST-2 cells transfected with siRNA for *Hivep1*, *Hivep2, or Hivep3* were analyzed by a microarray assay (supplemental Tables 2–4, respectively), and the results were com-

TABLE 1

Genes down-regulated by loss of the Hivep family genes

ST-2 cells were transfected with siRNA for *Hivep1*, *Hivep2*, or *Hivep3* and treated with BMP-2 (300 ng/ml) for 2 days. mRNA samples were subjected to microarray analysis. *A*, expression of five genes was commonly decreased by all the siRNAs for the three Hivep genes. *B*, expression of six genes was commonly down-regulated by the *Hivep1* and *Hivep2* siRNAs. *C*, expression of four genes was commonly down-regulated by the *Hivep1* and *Hivep3* siRNAs. *D*, expression of three genes was commonly down-regulated by the *Hivep2* and *Hivep3* siRNAs.

A

Unique Sorted Transcript ClusterID	siCont	siHivep1	siHivep2	siHivep3	gene symbol	gene description
17305520	21.529846	11.831301	9.75173	7.9562707	*Ear1*	eosinophil-associated, ribonuclease A family, member 1
17467150	24.856544	14.449716	11.51435	15.580148	*Vmn1r18*	vomeronasal 1 receptor 18
17444697	31.70125	19.534565	21.051311	17.505947	*Cyp3a59*	cytochrome P450, subfamily 3A, polypeptide 59
17245120	44.998398	29.873207	26.863188	29.873207	*1700030O20Rik*	RIKEN cDNA 1700030O20 gene
17481207	17.905426	10.739602	10.739602	10.603919	*Olfr608*	olfactory receptor 608

B

Unique Sorted Transcript ClusterID	siCont	siHivep1	siHivep2	gene symbol	gene description
17278822	65.41499	39.391872	41.367386	*Mir679*	microRNA 679
17302598	42.895184	26.84824	22.885633	*Gm6280*	predicted gene 6280
17344852	19.322012	12.227982	11.5472975	*Olfr97*	olfactory receptor 97
17509018	24.977375	16.012548	11.412771	*Adam34*	a disintegrin and metallopeptidase domain 34
17495404	82.13324	52.76455	42.29805	*Rps13*	ribosomal protein S13
17541719	21.694231	14.250495	14.178923	*Mir450-2*	microRNA 450-2

C

Unique Sorted Transcript ClusterID	siCont	siHivep1	siHivep3	gene symbol	gene description
17356739	63.32018	36.357323	32.77719	*Mir194-2*	microRNA 194-2
17268088	22.22885	13.294091	13.626566	*Gm11543*	predicted gene 11543
17324996	19.940779	12.472511	12.472511	*Mir1947*	microRNA 1947
17516159	30.844234	20.207043	19.56977	*Olfr251|Olfr900*	olfactory receptor 251 | olfactory receptor 900

D

Unique Sorted Transcript ClusterID	siCont	siHivep2	siHivep3	gene symbol	gene description
17395379	248.2335	129.81422	142.53452	*LOC100504873*	zinc finger protein 14-like
17320035	82.69005	51.436905	49.273067	*Mir1249*	microRNA 1249
17366886	162.14816	104.84351	90.903786	*Mir467e*	microRNA 467e

pared. The expression of five genes decreased in all three knockdown experiments (Table 1, *A*), whereas six genes, four genes, or three genes were down-regulated in common by siHivep1 and siHivep2 (Table 1, *B*), siHivep1 and siHivep3 (Table 1, *C*), or siHivep2 and siHivep3 (Table 1, *D*), respectively, although no trend was observed in the purified genes. Moreover, none of the purified genes was reported to correlate with differentiation of osteoblasts or chondrocytes. To investigate the roles and possible synergism of the Hivep genes in osteoblast differentiation, the expression of the three Hivep genes was knocked down in ST-2 cells, alone or in combination (Fig. 1*E*). Although combined genetic ablation of the *Hivep2* and *Hivep3* genes in mice resulted in synergistically increased bone formation and bone volume (17), siRNA-mediated silencing of *Hivep2* in BMP-2-stimulated ST-2 cells decreased the expression and activity of ALP (Fig. 1*E*, compare *lanes 2* and *4*), whereas loss of *Hivep3* alone enhanced the osteoblast differentiation (Fig. 1*E*, compare *lanes 2* and *5*). Interestingly, combined transfection of siHivep2 with siHivep3 negated the enhancement of ALP production by *Hivep3* knockdown (Fig. 1*E*, compare *lanes 2, 5,* and *8*). Similar to siHivep2, *Hivep1* siRNA inhibited ALP activity; however, there was no synergistic or additive effect on combined knockdown of *Hivep1* and *Hivep2*. These results suggest that, in ST-2 bone marrow stromal cells, the cell autonomous actions of Hivep genes are diverse and show no cooperation in osteoblast differentiation and that Hivep1 and Hivep2 promote the counteraction of the suppressive effect of Hivep3. In contrast, in an siRNA-mediated knockdown assay in ATDC5 chondrocytes, siHivep1, siHivep2, and siHivep3 all decreased the BMP-2-induced expression of the chondrocyte-specific type XI collagen gene (*Col11a2*) (Fig. 1*F*). A similar result was observed in another chondrocytic cell line, C3H10T1/2, where knockdown of both *Hivep2* and *Hivep3* decreased the level of a chondrocyte marker, type II collagen gene (*Col2a1*) (Fig. 1*G*). In both experiments in chondrogenic cells, the combined loss of the Hivep genes showed some additive effects.

Hivep3 Suppresses Osteoblast Differentiation in Vitro—Although the mRNA level of Runx2 was comparable between wild-type and Hivep3 knock-out cells, the protein levels of Runx2, as well as the mRNA levels of the early osteoblast differentiation markers osterix (*Sp7*), alkaline phosphatase (*Alpl*), activating transcription factor 4 (*Atf4*), and bone sialoprotein (*Ibsp*) and of the late maturation marker osteocalcin (*Bglap2*) increased in knock-out osteoblasts (10). We first checked if this effect could be reproduced via siRNA-mediated knockdown in osteoblastic cell lines. We used the mouse bone marrow stromal cell line ST-2 as a model for premature osteoblast progenitors and MC3T3-E1 mouse calvaria-derived osteoblasts as mature osteoblasts. In both MC3T3-E1 and ST-2 cells, ~50% knockdown was achieved by transfection of siHivep3 (Fig. 2, *A* and *C*). As expected, *Hivep3* silencing did not have any effect on the mRNA expression of *Runx2* (Fig. 2, *A* and *C*). In ST-2 cells treated with cycloheximide to block *de novo* synthesis of Runx2

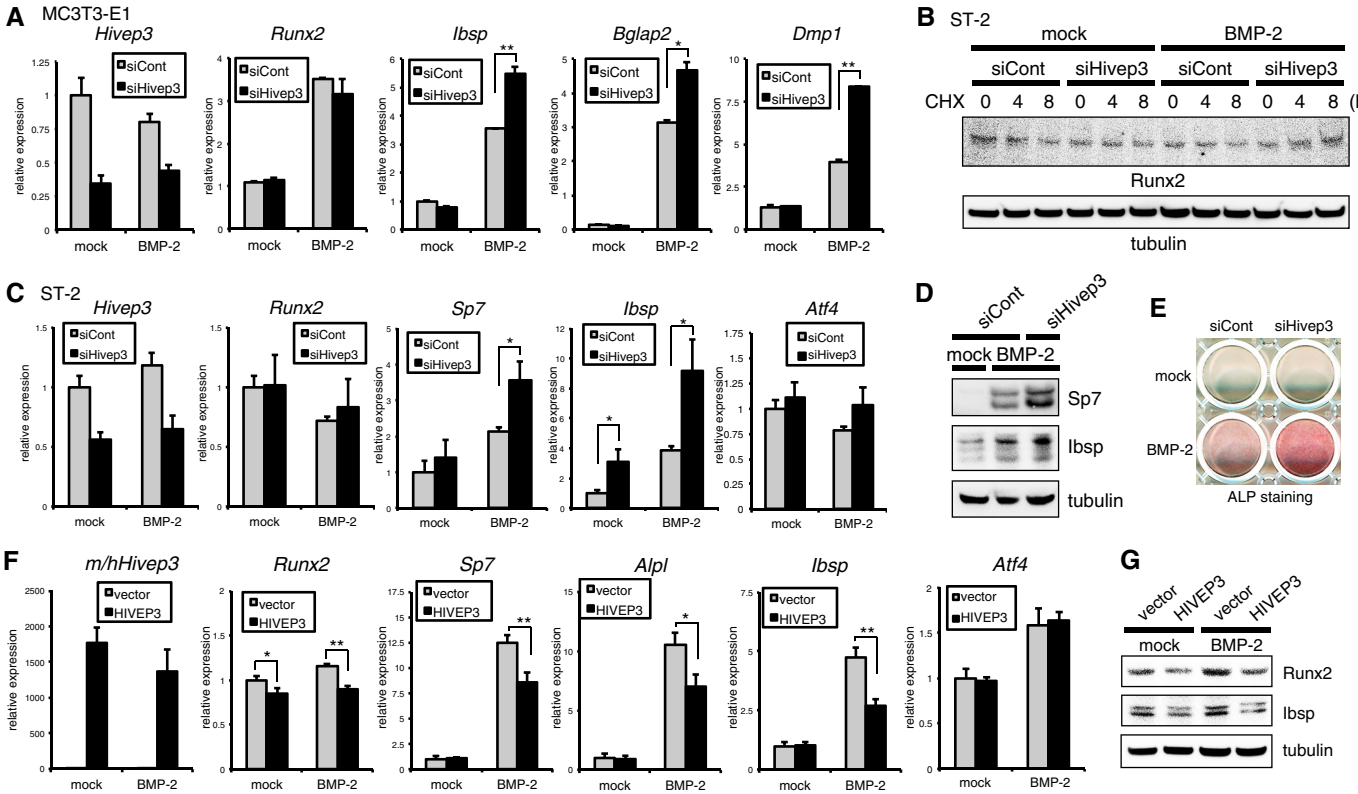

FIGURE 2. **Silencing of *Hivep3* increases protein stability of Runx2 to promote BMP-2-induced osteoblast differentiation.** *A*, MC3T3-E1 osteoblasts were transfected with siRNA for *Hivep3* with or without BMP-2 treatment (300 ng/ml) for 6 days. qRT-PCR analysis was performed for the indicated genes. *B*, siRNA-transfected ST-2 cells were treated with 100 μg/ml cycloheximide (*CHX*) with or without BMP-2 treatment (300 ng/ml) for the indicated time points. Cell lysates were analyzed by immunoblotting with an anti-Runx2 antibody. Tubulin served as a loading control. *C*, ST-2 cells were transfected with siRNA for *Hivep3* with or without BMP-2 treatment (300 ng/ml) for 3 days. The expression level of the indicated genes was examined by qRT-PCR. *D*, ST-2 cells were transfected with siRNA for *Hivep3* with BMP-2 treatment (300 ng/ml) for 7 days. Cell lysates were analyzed by immunoblotting with the indicated antibodies. Tubulin served as a loading control. *E*, ST-2 cells were transfected with *Hivep3* siRNA and stimulated with BMP-2 (300 ng/ml) for 6 days. ALP staining was performed. *F*, ST-2 cells were transfected with a human HIVEP3 expression vector and further stimulated with BMP-2 (300 ng/ml) for 4 days. The expression of the indicated genes was evaluated by qRT-PCR. *G*, ST-2 cells transfected with a human HIVEP3 expression vector were stimulated with BMP-2 (300 ng/ml) for 5 days. Cell lysates were analyzed by immunoblotting with the indicated antibodies. Tubulin served as a loading control. *, $p < 0.05$; **, $p < 0.01$.

protein, the protein level of Runx2 decreased in a time-dependent manner (Fig. 2*B*), although the protein expression was maintained in siHivep3-transfected cells. Moreover, combined induction of BMP-2 and siHivep3 in ST-2 cells increased Runx2 protein in a time-dependent fashion (Fig. 2*B*). Therefore, siRNA-mediated silencing of *Hivep3* stabilized Runx2 protein. As a result, expression of *Sp7*, *Ibsp*, and *Bglap2* was up-regulated in MC3T3-E1 and ST-2 cells (Fig. 2, *A* and *C*). In addition, the expression of an osteocyte marker, dentin matrix protein 1 (*Dmp1*), was elevated by *Hivep3* knockdown in MC3T3-E1 osteoblasts (Fig. 2*A*). The siHivep3-mediated increase of osteoblastic differentiation in ST-2 cells was confirmed by immunoblotting against Sp7 and Ibsp (Fig. 2*D*) or ALP staining (Fig. 2*E*). We introduced the human *HIVEP3* gene in ST-2 cells through transfection and confirmed the transgene expression by qRT-PCR (Fig. 2*F*). HIVEP3 suppressed BMP-2-induced osteoblast differentiation (Fig. 2, *F* and *G*) and protein expression of Runx2 (Fig. 2*G*). Interestingly, the mRNA expression of *Runx2* decreased following transfection with HIVEP3. As HIVEP3 destabilizes Runx2 protein, this result is likely due to loss of auto-induction of Runx2 (22), in which endogenous Runx2 mRNA expression increased in Runx2 transgenic mice (23). In both cases of knockdown and overexpression of *Hivep3*, expression of *Atf4* did not change (Fig. 2, *C* and *F*), although it increased in *Hivep3* knock-out osteoblasts (10).

Reduced Alg2 Gene Expression Following Knockdown of Hivep3—We next screened for genes whose expression was commonly reduced in both ST-2 cells and MC3T3-E1 cells upon *Hivep3* silencing by microarray analysis. The genes with decreased expression in MC3T3-E1 or ST-2 cells by >1.5-fold are listed in supplemental Table 5 (38 genes) or supplemental Table 4 (74 genes), respectively. Among these genes, only five were commonly down-regulated by siHivep3 in the two cell lines (Fig. 3*A*). For more stringent screening, we further increased the cutoff threshold to a >1.8-fold decrease, which left two genes each in the two cell lines, *Lypla2* and *Alg2* in MC3T3-E1 cells and *Alg2* and *Igfbp5* in ST-2 cells (Fig. 3*A*). Therefore, *Alg2* most commonly showed a decrease in expression due to *Hivep3* knockdown in both MC3T3-E1 and ST-2 cells. Asparagine-linked glycosylation (ALG) is one of the most common protein modification reactions in eukaryotic cells, as many proteins that are translocated across or integrated into the rough ER carry *N*-linked oligosaccharides (24). Alg2 is an α-1,3-mannosyltransferase forming a type I transmembrane protein on the ER, with its active site being cytosolically oriented (25). To date, no information has been reported to link

A

MC3T3-E1				
gene symbol	gene description	siCont	siHivep3	fold decrease
Lypla2	lysophospholipase 2	855.57886	385.55112	2.219106146
Alg2	**asparagine-linked glycosylation 2**	**1875.0286**	**875.0924**	**2.142663563**
Igfbp5	insulin-like growth factor binding protein 5	3540.0374	2207.5708	1.60358952
Ankfy1	ankyrin repeat and FYVE domain containing 1	1102.1857	719.4798	1.531920285
Gpr133	G protein-coupled receptor 133	545.9816	362.30106	1.50698317

ST-2				
gene symbol	gene description	siCont	siHivep3	fold decrease
Alg2	**asparagine-linked glycosylation 2**	**568.02734**	**314.0774**	**1.808558464**
Igfbp5	insulin-like growth factor binding protein 5	179.31311	99.23038	1.807038429
Lypla2	lysophospholipase 2	586.02966	349.82162	1.675224247
Ankfy1	ankyrin repeat and FYVE domain containing 1	1006.6627	650.5681	1.547359454
Gpr133	G protein-coupled receptor 133	93.81231	61.831158	1.517233593

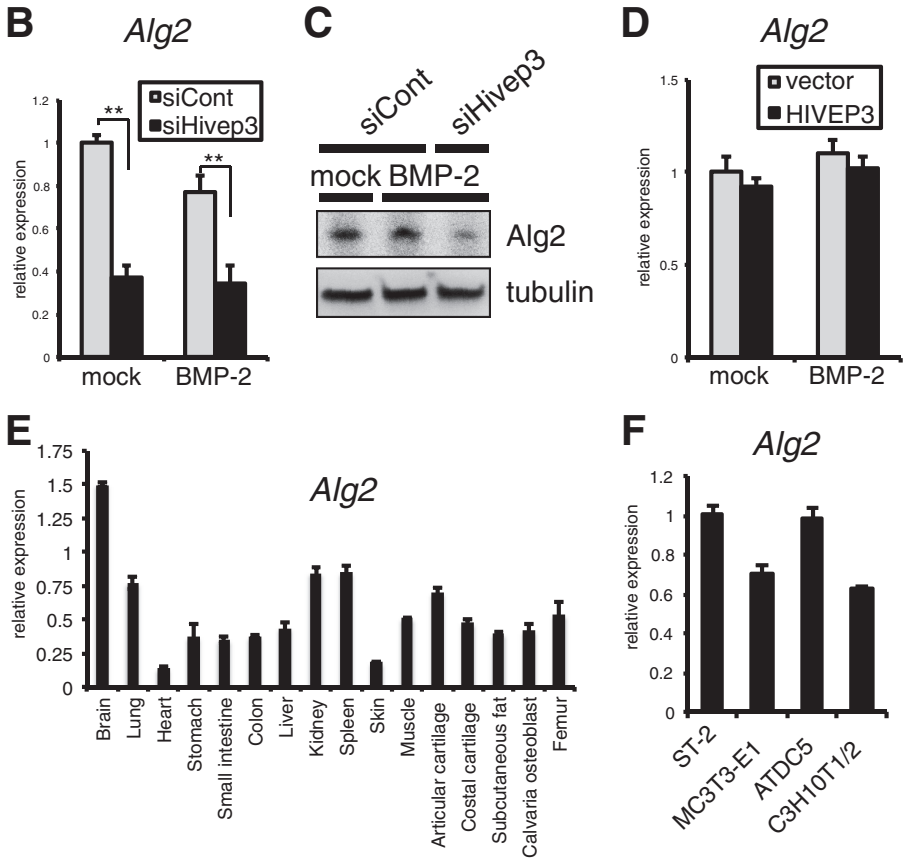

FIGURE 3. **Expression of the *Alg2* gene is reduced upon knockdown of *Hivep3* in osteoblastic cells.** *A*, siRNA for *Hivep3* was transfected into MC3T3-E1 or ST-2 cells prior to treatment with BMP-2 (300 ng/ml) for 2 days and analyzed by microarray. A list of five genes with decreased signal intensity, in common between MC3T3-E1 and ST-2 cells, is presented. *B*, ST-2 cells were transfected with siRNA for *Hivep3* with or without BMP-2 treatment (300 ng/ml) for 3 days. The expression level of *Alg2* was examined by qRT-PCR. *C*, ST-2 cells were transfected with siRNA for *Hivep3* with BMP-2 treatment (300 ng/ml) for 7 days. Cell lysates were analyzed by immunoblotting with an anti-Alg2 antibody. Tubulin served as a loading control. *D*, ST-2 cells were transfected with a human HIVEP3 expression vector to be stimulated with BMP-2 (300 ng/ml) for 4 days. The expression of *Alg2* was evaluated by qRT-PCR. *E*, tissue cDNA panel of a 3-month-old mouse was subjected to real time PCR for *Alg2*. *F*, expression level of *Alg2* in the indicated cell lines was examined by a qRT-PCR assay. **, $p < 0.01$.

Alg2 to cell differentiation. We confirmed the microarray results by qRT-PCR (Fig. 3*B*) or immunoblotting (Fig. 3*C*) and verified that knockdown of *Hivep3* in ST-2 cells decreased the level of *Alg2* by over 50%. However, forced expression of HIVEP3 did not increase *Alg2* expression (Fig. 3*D*). We next examined the tissue distribution of *Alg2* in 3-month-old mice by quantitative PCR analysis of a tissue cDNA panel (Fig. 3*E*). In tissues with low expression of *Hivep3* (Fig. 1*C*), *i.e.* the heart or skin, *Alg2* also showed a minimum level of expression, although both genes were highly expressed in the brain and lungs, suggesting a linkage between the levels of the two genes. However, there were some exceptions, *e.g. Hivep3* was expressed at high levels in fat, cartilage, and bone, whereas *Alg2* was detected at a moderate level in these tissues. From the osteoblastic and/or chondrocytic cell lines, MC3T3-E1 showed a significantly high level of *Hivep3* expression (Fig. 1*D*), whereas *Alg2* was detected in a relatively ubiquitous pattern (Fig. 3*F*). These results suggest that Hivep3 is essential but not sufficient for the expression of *Alg2*.

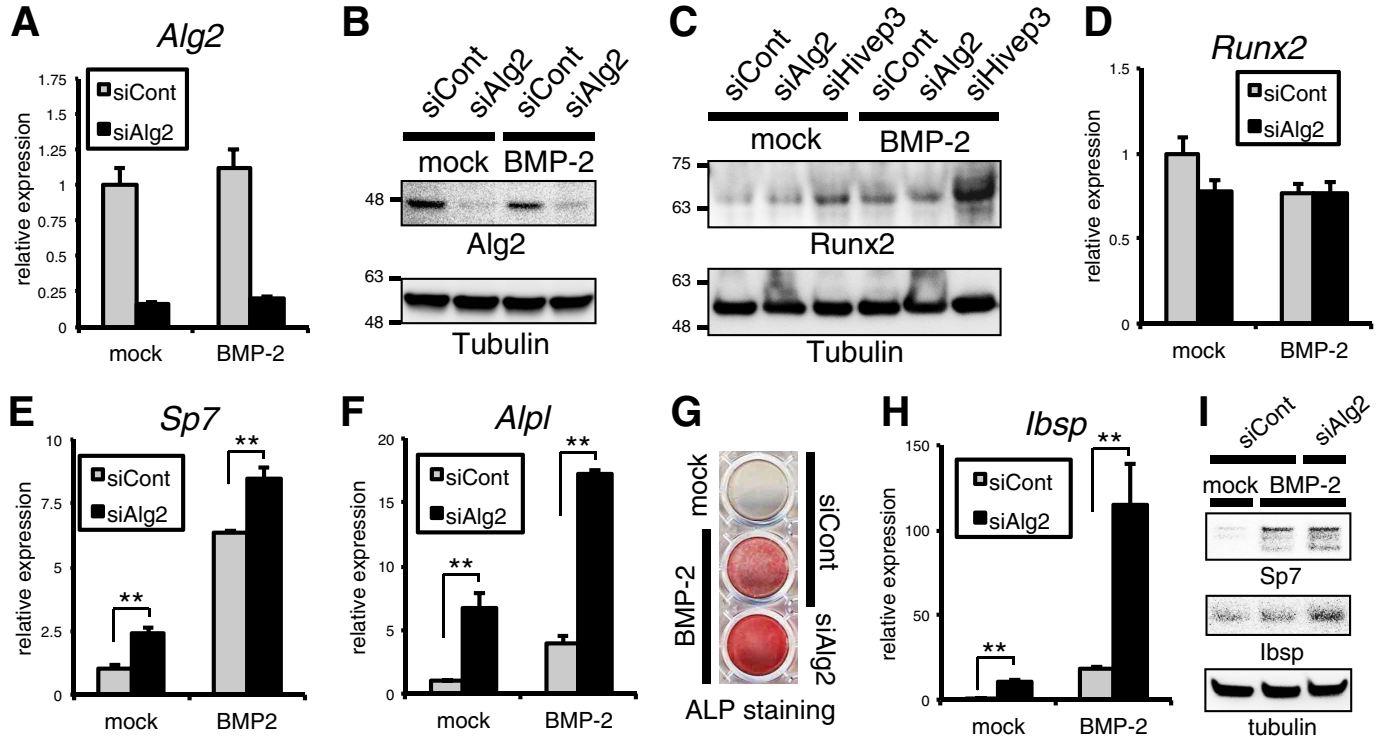

FIGURE 4. **Loss of Alg2 enhances osteoblast differentiation in ST-2 cells without affecting the protein level of Runx2.** *A* and *B*, ST-2 cells were transfected with siRNA for *Alg2* with or without BMP-2 treatment (300 ng/ml) for 3 days. Knockdown efficiency for *Alg2* was examined by qRT-PCR (*A*) or by immunoblotting (*B*). *C*, ST-2 cells were transfected with siRNA for *Alg2* or *Hivep3* with or without BMP-2 treatment (300 ng/ml) for 3 days. Cell lysates were analyzed by immunoblotting with an anti-Runx2 antibody. Tubulin served as a loading control. *D–F*, ST-2 cells were transfected with siRNA for *Alg2* with or without BMP-2 treatment (300 ng/ml) for 3 days. Expression of indicated genes was analyzed by qRT-PCR. *G*, ST-2 cells were transfected with siRNA for *Alg2* and treated with BMP-2 (300 ng/ml) for 6 days. ALP staining was performed. *H*, ST-2 cells were transfected with siRNA for *Alg2* with or without BMP-2 treatment (300 ng/ml) for 3 days. Expression of *Ibsp* was analyzed by qRT-PCR. *I*, ST-2 cells were transfected with siRNA for *Alg2* with BMP-2 treatment (300 ng/ml) for 2 days. Cell lysates were analyzed by immunoblotting with indicated antibodies. **, $p < 0.01$.

Loss of Alg2 Promotes Osteoblast Differentiation in ST-2 Cells without Affecting the Protein Level of Runx2—To investigate the possible role of Alg2 in osteoblast differentiation, siRNA for *Alg2* was transfected into ST-2 cells to obtain an ~80% decrease in mRNA expression (Fig. 4*A*) and in protein level (Fig. 4*B*). Although silencing of *Hivep3* increased the level of Runx2 protein, siAlg2 had no effect (Fig. 4*C*). As expected, loss of Alg2 also did not change the RNA level of Runx2 (Fig. 4*D*). However, *Alg2* knockdown mildly enhanced *Sp7* expression (Fig. 4, *E* and *I*), although it dramatically increased the expression (Fig. 4*F*) and activity (Fig. 4*G*) of ALP. A similar effect was seen on the level of *Ibsp* mRNA (Fig. 4*H*) and protein (Fig. 4*I*), suggesting a suppressive role of Alg2 in osteoblast maturation.

Forced Expression of Alg2 Inhibits Osteoblast Differentiation and Bone Formation—We investigated the effect of overexpression of Alg2 in osteoblasts by infection of adenovirus or lentivirus carrying an Alg2 expression cassette. In ST-2 cells, forced expression of Alg2 showed no effect on Runx2 protein level (Fig. 5*A*), whereas it strongly suppressed the expression of *Sp7*, *Alpl*, and *Ibsp* (Fig. 5*B*). The lentivirus-mediated expression of the Alg2 transgene product was confirmed at the protein and mRNA level (Fig. 5, *C* and *D*). Combined induction of *Hivep3* siRNA with the Alg2 lentivirus completely negated the enhanced expression of *Ibsp* by siHivep3, suggesting that Alg2 is a downstream mediator of Hivep3 for blocking osteoblast differentiation (Fig. 5*E*). To assess the role of Alg2 in osteoblastic bone formation, we employed the *ex vivo* culture system of calvarial bone harvested from E17.5 mouse embryo. The infection efficiency of lentivirus in bone culture was evaluated by immunofluorescence, and the V5-tagged transgene product was detected by anti-V5 antibody (Fig. 5*F*). The rate of osteoblastic intramembranous bone formation can be examined by measuring the width of the fontanelle (20). Application of BMP-2 promoted the bone formation, and it significantly decreased the fontanelle width, whereas combined induction of Alg2-expressing lentivirus cancelled the narrowing (Fig. 5*G*), indicating that Alg2 inhibited BMP-induced osteoblastic bone formation.

Alg2 Knockdown Does Not Affect ER Stress nor BMP Signaling in ST-2 Cells—A defect in ALG may affect the quality control of protein folding in the ER, which might subsequently evoke ER stress (26, 27). In addition, because physiologically mild ER stress is required for proper osteoblast differentiation and maturation (28, 29), we investigated the effect of *Alg2* siRNA on ER stress-related genes by qRT-PCR (Fig. 6*A*). Atf4, a downstream target of PKR-like endoplasmic reticulum kinase of ER stress transducer, is crucial for the expression of *Bglap2* and synthesis of type I collagen during osteoblast maturation (28, 30). *Alg2* silencing showed no remarkable effect on the *Atf4* mRNA level (Fig. 6*A*). An ER stress transducer called cAMP-responsive element-binding protein 3-like 1 (*Creb3l1*), alternatively known as Oasis, is also crucial in osteoblast differentiation (29). However, the level of *Creb3l1* was unchanged by Alg2 silencing (Fig. 6*A*). DNA damage-inducible transcript 3 (*Ddit3*), a target gene of

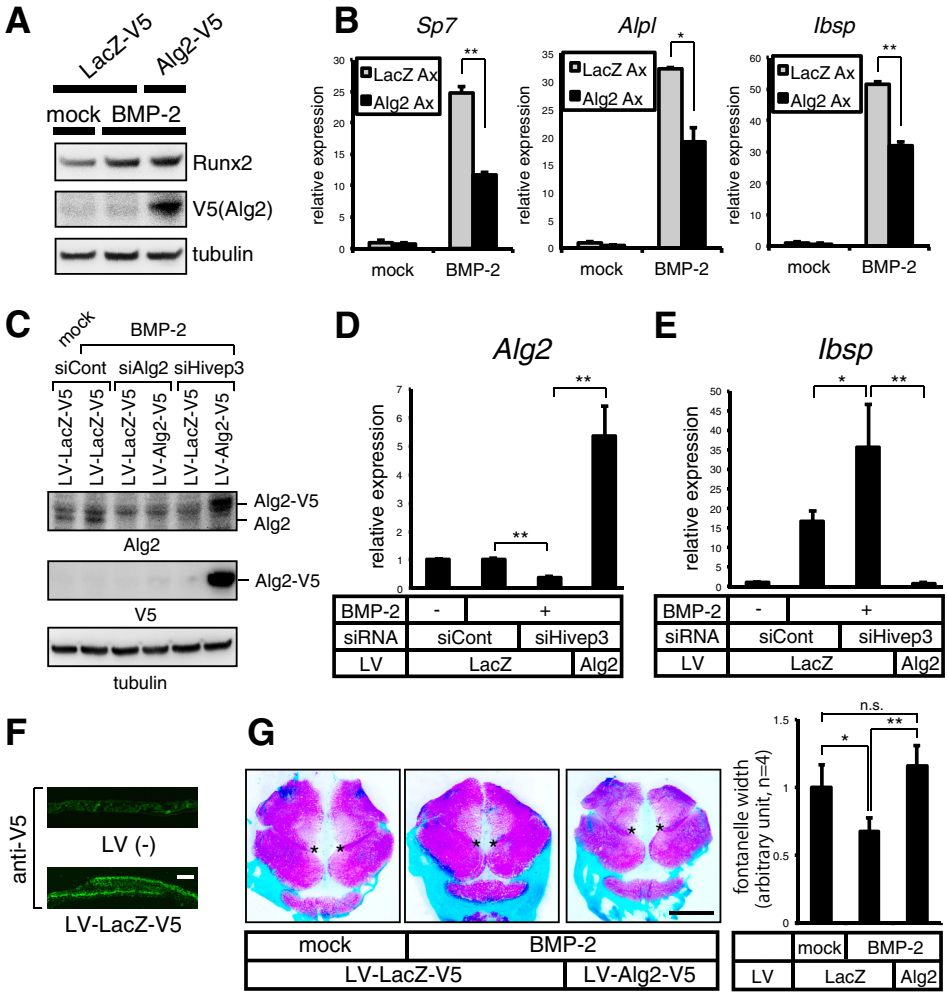

FIGURE 5. **Gain of Alg2 expression suppresses osteoblast differentiation and bone formation.** *A* and *B*, ST-2 cells were infected with V5-tagged LacZ or Alg2 adenovirus (*Ax*) and subsequently treated with BMP-2 (300 ng/ml). Cell lysates were analyzed by immunoblotting with anti-Runx2 and anti-V5 antibodies at day 6 (*A*). The expression of the indicated genes was evaluated by qRT-PCR (*B*). *C–E*, ST-2 cells were infected with LacZ or Alg2 lentivirus (*LV*). The infectants were transfected with the indicated siRNAs and stimulated with BMP-2 (300 ng/ml) for 4 days before analysis by immunoblotting with anti-Alg2 or anti-V5 antibodies (*C*). Expression of *Alg2* (*D*) or *Ibsp* (*E*) was evaluated by qRT-PCR. *F* and *G*, calvarial bones of E17.5 mouse embryos were infected with the indicated lentivirus for 16 h. Immunostaining using FITC-linked anti-V5 antibody on bone coronal sections was performed at day 2 of culture (*F*). *Scale bar,* 100 μm. LV-infected bones were treated with 300 ng/ml of BMP-2 for 3 days. Alcian blue/alizarin red staining was performed. The width of fontanelle (between *asterisks*) was measured (*G*). *Scale bar*, 2 mm. *, $p < 0.05$; **, $p < 0.01$.

Atf4 also known as CCAAT/enhancer-binding protein homologous protein (Chop), was indeed mildly up-regulated by siAlg2, but only in BMP-2-treated cells (Fig. 6*A*). The expression of a target of the Atf6 pathway, heat shock protein 5 (*Hspa5*), also known as Bip, was not altered by loss of Alg2 (Fig. 6*A*). These data suggest that ER stress is not substantially accelerated by loss of Alg2. To identify other mechanisms by which siAlg2 promotes osteoblast differentiation, we next evaluated if BMP signaling was increased by Alg2 knockdown, by assessing the expression of the representative direct target genes of the BMP-Smad pathway, *Id1* and *Smad6* (31, 32). We found no change in the level of *Id1* or *Smad6* upon Alg2 silencing (Fig. 6*B*).

Alg2 Interferes with the Transcriptional Activity and Nuclear Localization of Runx2—To test whether Alg2 interferes with Runx2 activity, we analyzed a Runx2-binding 6×OSE2 luciferase reporter. We found that Alg2 dose-dependently suppressed the Runx2-induced elevation of luciferase activity in COS-7 cells, whereas it showed no effect on the activity of 6×OSE2 reporter with Runx2-binding site mutation, suggesting that the inhibitory effect was Runx2-dependent (Fig. 6*C*). A similar result was obtained in ST-2 cells where Alg2 reduced Runx2 activity with an efficiency comparable with that of Hivep3 (Fig. 6*D*). To investigate the mechanism by which Alg2 suppresses Runx2 activity, we examined the impact of siAlg2 on the expression of an inhibitor and an activator of Runx2. Hairy/enhancer-of-split related with YRPW motif 1 (*Hey1*) is a transcriptional repressor that binds to Runx2 and suppresses its transcriptional activity (33). Contrary to our hypothesis, the expression of *Hey1* was not decreased by Alg2 knockdown; rather, it increased in a statistically significant manner (Fig. 6*E*). The expression of hairy and enhancer of split 1 (*Hes1*), which forms a complex with Runx2 to promote Runx2-dependent transcription (34, 35), was found to be unchanged by Alg2 siRNA (Fig. 6*E*). We next investigated the possibility of whether Alg2 forms a complex with Runx2 to interfere with its localization, because targeting of Runx2 to subnuclear foci, the nuclear matrix, is crucial for the bone-specific transcription of Runx2

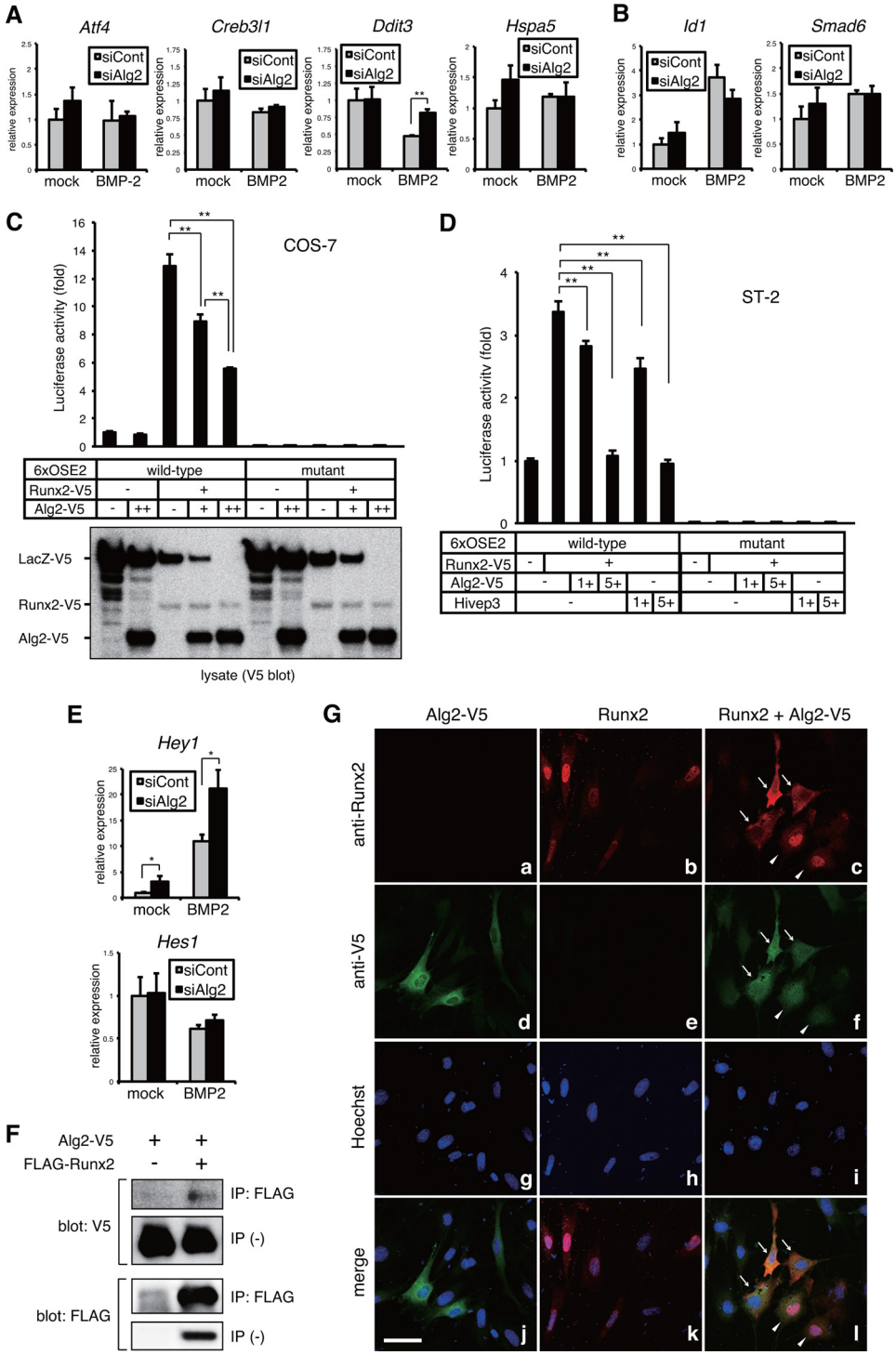

FIGURE 6. **Alg2 suppresses the transcriptional activity of Runx2.** *A* and *B*, ST-2 cells were transfected with siRNA for *Alg2* and treated with or without BMP-2 (300 ng/ml) for 3 days. Expression of indicated genes was analyzed by qRT-PCR. *C* and *D*, a luciferase reporter, 6×OSE2 luc or a Runx2-binding sequence mutant 6×OSE2 luc, and a Runx2 expression vector were transfected with or without Alg2 or Hivep3 expression plasmid into COS-7 cells (*C*) or ST-2 cells (*D*) and examined by a luciferase assay. Protein expression from the transgenes was confirmed by anti-V5 immunoblotting (*C*). *E*, ST-2 cells were transfected with siRNA for *Alg2* and treated with or without BMP-2 (300 ng/ml) for 3 days. Expression of *Hey1* and *Hes1* was analyzed by qRT-PCR. *F*, COS-7 cells were transfected with a V5-tagged Alg2 expression plasmid with or without a FLAG-tagged Runx2 vector. The cell lysate was subjected to immunoprecipitation (*IP*) with an anti-FLAG antibody and subsequent immunoblotting with an anti-V5 or anti-FLAG antibody. *G*, ST-2 cells were transfected with a V5-tagged Alg2 plasmid and/or a Runx2 expression vector. Immunofluorescence was examined with anti-Runx2 or anti-V5 antibodies. Nuclei were stained with Hoechst dye. *Scale bar,* 50 μm. *, $p < 0.05$; **, $p < 0.01$.

(36). In a co-transfection experiment using COS-7 cells, Alg2 was immunoprecipitated with Runx2 (Fig. 6*F*). By an immunofluorescence assay in ST-2 cells, we found that Alg2 protein overexpressed alone was localized to the ER (Fig. 6*G*, *panel d*), whereas Runx2 overexpressed alone was stained in the nuclei (Fig. 6*G*, *panel b*). However, in cells with combined transfection of Alg2 and Runx2, in the portion of cells in which abundant expression of Alg2 was observed, Runx2 was excluded from

nucleus and co-localized with Alg2 in the cytoplasm (*arrows*), whereas cells with a lower level of Alg2 had a nuclear pattern of Runx2 staining (*arrowheads*) (Fig. 6*G*, *panels c, f,* and *l*). These data suggest that the interaction of Runx2 with Alg2 interfered with proper subnuclear localization of Runx2, thereby decreasing its transcriptional activity.

Hivep3 Promotes the Expression of Creb3l2 and Differentiation of Chondrocytes—Next we investigated the mechanism by which Hivep3 supports chondrocyte differentiation. *Hivep3* silencing in ATDC5 chondrocytes strongly suppressed *Col2a1* in mRNA (Fig. 7*A*) and in protein levels (Fig. 7*B*). Conversely, HIVEP3 overexpression significantly enhanced expression of *Col2a1* (Fig. 7*C*). At day 21 of micromass culture, BMP-2-treated ATDC5 cells produced an abundant cartilage matrix that was stained with Alcian blue and was significantly enlarged by Hivep3 vector transfection (Fig. 7*D*). Chondrocytes secrete cartilage ECM proteins such as type II or XI collagens during differentiation, which evokes mild ER stress and induces an ER stress sensor, BBF2 human homolog on chromosome 7 (*Bbf2h7*), also known as Creb3l2. Creb3l2 plays a crucial supportive role in chondrocyte differentiation by directly inducing the expression of *Sec23a*, encoding a coat protein complex II component cargo protein responsible for the transport of secretory ECM proteins from the ER to the Golgi (18). *Atf4* expression was increased by loss of Hivep3, but only in the absence of BMP-2 (Fig. 7*E*), although gain of HIVEP3 enhanced the level in the presence of BMP-2 (Fig. 7*F*). *Ddit3* showed similar expression patterns as *Atf4*, where its basal level was elevated by siHivep3 (Fig. 7*G*), although overexpression of HIVEP3 suppressed basal expression but promoted expression in the presence of BMP-2 (Fig. 7*H*). These data indicate that the ER stress pathway of PERK-Atf4-Chop may be associated with the enhancement of BMP-2-induced differentiation by forced expression of HIVEP3. Expression of *Hspa5* was decreased or increased by knockdown or overexpression of Hivep3, respectively (Fig. 7, *I* and *J*). The expression of a spliced form of *Xbp1* was examined to monitor the inositol-requiring 1 (IRE1) pathway of ER stress and found to be suppressed or enhanced by silencing or addition of Hivep3, respectively (Fig. 7, *K* and *L*). These data suggest that Hivep3 evoked mild ER stress through the Atf6-Bip and Ire1-Xbp1 pathways. We found that *Creb3l2* expression was decreased or increased by loss or gain of Hivep3, respectively (Fig. 7, *M* and *N*). Importantly, the siHivep3-mediated reduction in *Creb3l2* expression was reflected in that of *Sec23a* (Fig. 7*O*), which may be responsible for the inhibition of differentiation.

Alg2 Is Decreased by Hivep3 Silencing in ATDC5 Chondrocytes, although Loss of Alg2 Suppresses the Expression of Creb3l2 and Chondrocyte Differentiation—We investigated whether Alg2 is a mediator of Hivep3 also in chondrocytes to affect differentiation. Indeed, knockdown of *Hivep3* strongly suppressed the expression of *Alg2* in ATDC5 chondrocytes (Fig. 8*A*). Moreover, *Alg2* siRNA inhibited the BMP-2-induced expression of type II collagen in mRNA (Fig. 8*B*) and in protein level (Fig. 8*C*). We checked whether the loss of Alg2 evoked ER stress and that the basal expression of *Atf4* (Fig. 8*D*) and *Hspa5* (Fig. 8*F*) decreased, whereas *Ddit3* expression increased in the presence of BMP-2 (Fig. 8*E*), following siAlg2 transfection. Importantly, *Creb3l2* was down-regulated by *Alg2* silencing (Fig. 8*G*), and silencing of *Alg2* or *Hivep3* both diminished the band of Creb3l2 in immunoblotting (Fig. 8*H*). Finally, we infected Alg2-expressing adenovirus in cultured mouse metatarsal cartilage, because this *ex vivo* organ culture is an excellent system to evaluate the rate of chondrocyte maturation (37). Indeed, application of BMP-2 into this cartilage culture promoted the calcification of cartilage matrix by mature hypertrophic chondrocytes (Fig. 8*J*, *1st* and *3rd lanes*). The infection efficiency of adenovirus was evaluated by immunofluorescence, and the V5-tagged transgene product was detected by anti-V5 antibody in the cartilage sample (Fig. 8*I*). Importantly, Alg2-expressing adenovirus mildly but significantly increased the zone of mature chondrocytes regardless of BMP-2 treatment (Fig. 8*J*), indicating that Alg2 promotes cartilage maturation. Taken together, these data suggest that Alg2, induced by Hivep3, is necessary for the induction of *Creb3l2* to promote chondrogenesis.

DISCUSSION

Drosophila Schnurri was one of the first partners identified for BMP-specific Smads (38, 39) for positive or negative regulation of BMP signaling. The structure of three Schnurri homologs in vertebrates, Hivep1, Hivep2, and Hivep3, is also similar to that of the fly Schnurri and shares additional features, including an unusually large size (~2500 amino acids) and acidic domains. We initially hypothesized that Hivep3 may inhibit BMP signaling to suppress osteoblast differentiation; however, the expression of the direct target genes of the BMP-Smad pathway, *Id1* or *Smad6*, was not altered by *Hivep3* knockdown in osteoblasts (data not shown). In this study, we found that the *Alg2* gene was commonly down-regulated in both ST-2 and MC3T3-E1 osteoblasts by *Hivep3* knockdown. Alg2 inhibited the activity of Runx2 without affecting its protein expression unlike Hivep3. Therefore, the Hivep3-Alg2 pathway efficiently blocks Runx2-mediated transcription and subsequent osteoblast differentiation by two approaches, regulation of protein degradation and intracellular localization. In ATDC5 chondrocytes, Alg2 expression was also controlled by Hivep3 to support chondrocyte differentiation (*Col2a1* expression), but its possible actions against Runx2 in chondrocytes remain elusive. Because Runx2 is directly crucial for transcription of the chondrocyte maturation marker gene type X collagen (*Col10a1*) in promoting chondrocyte hypertrophy (40), loss of Hivep3 or Alg2 may increase expression of *Col10a1* if they target Runx2 in chondrocytes. However, because expression of *Col10a1* arises sequentially after expression of early markers such as *Col2a1* or *Col11a2*, which had diminished expression in response to transfection with siRNA for *Hivep3* or *Alg2*, we could not clearly evaluate their effect on *Col10a1* expression (data not shown). Indeed, in *Hivep2*/*Hivep3* double knock-out mice, hypertrophic chondrocytes as well as expression of *Col10a1* have been found to decrease in the growth plates of long bones (17). Our data and those of other researchers suggest that Runx2 is not the target of Hivep3 in chondrocytes.

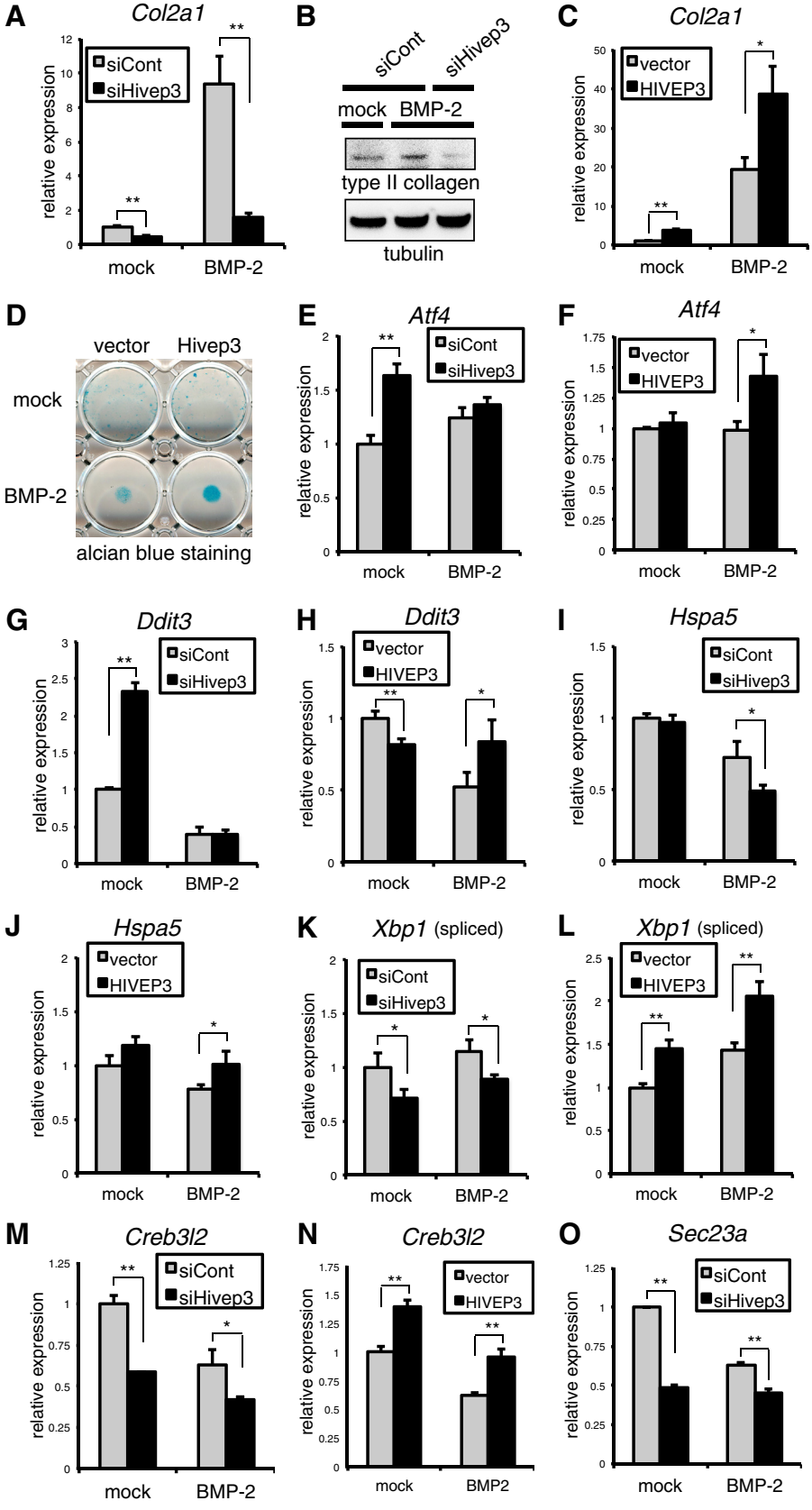
A
Col2a1
relative expression
siCont
siHivep3
mock
BMP-2
B
siCont
siHivep3
mock BMP-2
type II collagen
tubulin
C
Col2a1
vector
HIVEP3
D
vector Hivep3
mock
BMP-2
alcian blue staining
E
Atf4
F
Atf4
G
Ddit3
H
Ddit3
I
Hspa5
J
Hspa5
K
Xbp1 (spliced)
L
Xbp1 (spliced)
M
Creb3l2
N
Creb3l2
BMP2
O
Sec23a

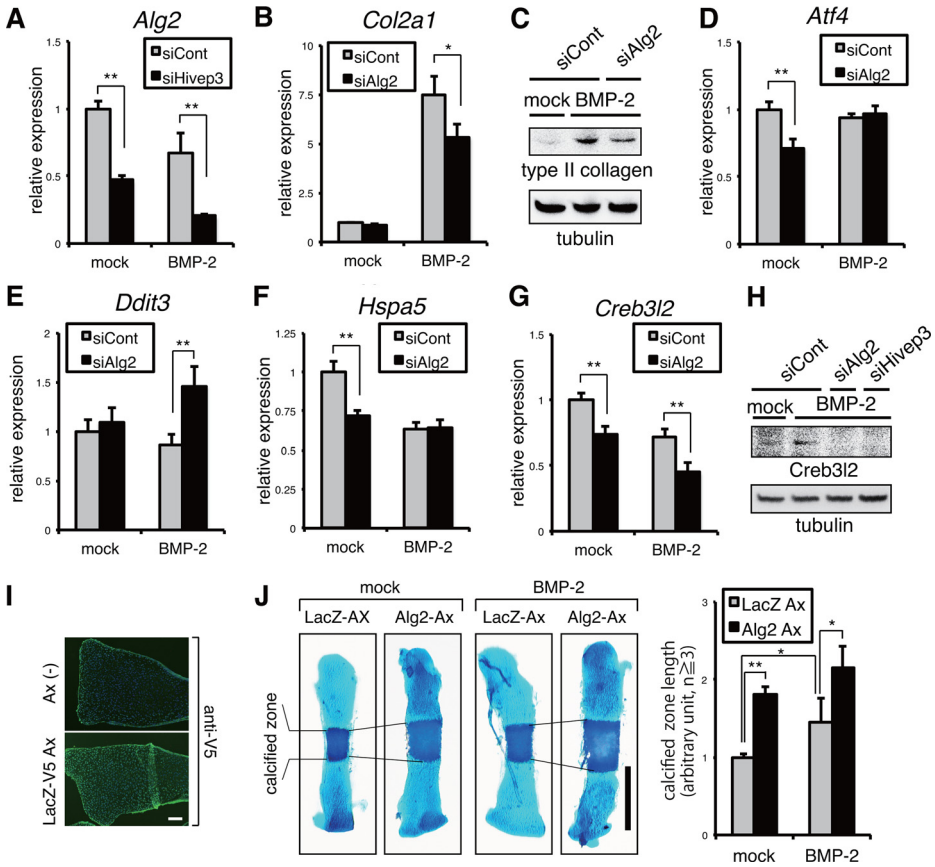

FIGURE 8. **Hivep3 is essential for Alg2 expression in ATDC5 chondrocytes, althoughAlg2 promotes chondrogenesis.** *A*, ATDC5 cells were transfected with siRNA for *Hivep3* and treated with BMP-2 (300 ng/ml) for 4 days. Expression of *Alg2* was evaluated by qRT-PCR. *B*, *D*, *E*, *F* and *G*, ATDC5 cells were transfected with siRNA for *Alg2* and treated with BMP-2 (300 ng/ml) for 4 days. The expression of the indicated genes was analyzed by qRT-PCR. *C*, ATDC5 chondrocytes were transfected with siRNA for *Alg2* with BMP-2 treatment (300 ng/ml) for 7 days. Cell lysates were analyzed by immunoblotting with an anti-type II collagen antibody. Tubulin served as a loading control. *H*, ATDC5 chondrocytes were transfected with siRNA for *Alg2* or *Hivep3* with BMP-2 treatment (300 ng/ml) for 3 days. Cell lysates were analyzed by immunoblotting with an anti-Creb3l2 antibody. Tubulin served as a loading control. *I* and *J*, metatarsal cartilages of E17.5 mouse embryos were infected with indicated adenovirus for 16 h. Immunostaining using FITC-linked anti-V5 antibody on bone coronal sections was performed at day 2 of culture (*I*). Nuclei were stained with Hoechst dye. Merged images are presented. *Scale bar,* 100 μm. Alcian blue/alizarin red staining was performed at day 3 of BMP-2 treatment (*J*). The length of calcified zone (matured hypertrophic chondrocytes) was measured. *Scale bar,* 500 μm. *, $p < 0.05$; **, $p < 0.01$.

Mutations in the *ALG2* gene cause the rarest form of congenital disorders of glycosylation (CDG) in humans, CDG type-Ii (CDG-Ii) (25). A single patient of CDG-Ii has been identified, who was only mildly affected with developmental delay, seizures, poor vision, coagulopathy, and delayed myelinization (25), with no remarkable bone phenotype. However, because the reported patient was 3 years old, and *Hivep3* knock-out mice have been reported to show adult-onset osteosclerosis (10), skeletal disorders may develop during the adulthood of the CDG-Ii patient. The glycosyltransferase enzymes of the ALG pathway use nucleotide- or dolichol-activated monosaccharides as donor substrates (41), which are biosynthesized by the cytosolic enzyme PMM2. CDG-Ia is the largest group of CDG cases with more than 800 patients who have been identified as having mutations in the *PMM2* gene (41). It is noteworthy that CDG-Ia patients show a variety of skeletal phenotypes, including osteopenia, rhizomelia, and ossification delay of bones (42). Fibrillar collagens, such as type I or type II collagens, are found predominantly in the ECM of bone or cartilage, respectively, and mature through ALG of the C-terminal pro-collagen, resulting in cleavage of the N- and C-terminal pro-peptide domains. Therefore, dysregulation of ALG may affect the maturation and function of collagens in the skeleton. Conversely, during the differentiation of osteoblasts and chondrocytes, nascent ECM protein is delivered in amounts that exceed the capacity of the ER, whose machinery processes the post-translational modifications and folding of proteins; ALG proteins play important roles for these steps. Such events of "overload" trigger mild ER stress (physiological ER stress) (43). In ST-2 cells, loss of Hivep3 did not influence mild ER stress during

FIGURE 7. **Hivep3 potentiates the physiological mild ER stress to promote chondrocyte differentiation.** *A*, *E*, *G*, *I*, *K*, *M*, and *O*, ATDC5 cells were transfected with siRNA for *Hivep3* and treated with BMP-2 (300 ng/ml) for 4 days. The expression of the indicated genes was evaluated by qRT-PCR. *B*, ATDC5 chondrocytes were transfected with siRNA for *Hivep3* with BMP-2 treatment (300 ng/ml) for 7 days. Cell lysates were analyzed by immunoblotting with an anti-type II collagen antibody. Tubulin served as a loading control. *C*, *F*, *H*, *J*, *L*, and *N*, ATDC5 cells were transfected with a human HIVEP3 expression vector and further stimulated with BMP-2 (300 ng/ml) for 4 days. The expression of the indicated genes was evaluated by qRT-PCR. *D*, ATDC5 cells were stably transfected with a pEF-Shn3 (*Hivep3*) expression vector. Micromass culture of the transfectants was treated with BMP-2 (300 ng/ml) for 21 days and stained with Alcian blue dye. *, $p < 0.05$; **, $p < 0.01$.

osteoblast differentiation. In contrast, Hivep3 increased not only the level of *Creb3l2*, but also of other canonical ER stress-related genes in ATDC5 chondrocytes, although loss of *Alg2* decreased the expression of *Creb3l2*. These results suggest that the Hivep3-Alg2 pathway is important for physiological ER stress in chondrocytes.

Although Hivep2 and Hivep3 showed cooperative roles in decreasing bone formation and bone volume *in vivo* (17), Saita *et al.* (16) reported results similar to ours where gain of Hivep2 expression enhanced osteoblast differentiation, and Hivep2 knock-out osteoblasts failed to support efficient osteoclastogenesis *in vitro*. In addition, they showed that bone formation, as well as bone resorption, decreased in the bones of Hivep2-null mice, resulting in osteopenia due to the low turnover of bone remodeling. Recently, Hivep3 was also found to promote osteoclastogenesis (14, 15). Taken together, the defects in osteoclastogenesis induced by loss of the Hivep genes seem to be mainly responsible for the additively increased bone volume in *Hivep2*/*Hivep3* double knock-out mice. In contrast, we showed that each of the three Hivep genes was essential for chondrogenesis *in vitro*, suggesting that the chondrodysplasia observed following combined ablation of Hivep2 and Hivep3 in mice (17) was a result of the loss of the cell autonomous action of the Hivep proteins. Although we found the physiological ER stress and the level of *Creb3l2* to be increased by the Hivep3-Alg2 axis, the precise molecular mechanisms are unclear. Moreover, it is still unclear why the three Hivep genes exhibit diverse actions in osteogenesis. Because expression of *Alg2* was not altered by loss of Hivep1 or Hivep2, other molecular targets downstream of Hivep1 or Hivep2 should be evaluated. Although Hivep proteins are known to act as transcription factors as well as scaffolds, they may harbor some other unknown properties, as most of the area of the large proteins has not been classified into any known functional domains.

In conclusion, Alg2 is a downstream mediator of Hivep3 in osteoblasts and chondrocytes. In addition to initiation of Runx2 protein degradation, Hivep3 interfered with the function of Runx2 via Alg2-mediated disturbance of localization and activity. In ATDC5 chondrocytes, Hivep3 and Alg2 enhanced mild ER stress to promote differentiation. Thus, our results are the first to link the ALG gene to differentiation of skeletal cells. Future studies on mice with knock-out of ALG genes, as well as detailed clinical research with corresponding CDG patients, may provide more information regarding the roles of ALG proteins in osteogenesis, chondrogenesis, and bone remodeling.

Acknowledgments—The pEF-Shn3(Hivep3) expression vector was kindly provided by Dr. Laurie Glimcher. The mouse type II Runx2 expression plasmid and 6×OSE2 luciferase plasmid were kind gifts from Dr. Toshihisa Komori. The mutant 6×OSE2 luciferase plasmid was a kind gift from Dr. Gerard Karsenty. We gratefully acknowledge the technical assistance of Hui Gao.

REFERENCES

1. Kronenberg, H. M. (2003) Developmental regulation of the growth plate. *Nature* **423,** 332–336
2. Boyle, W. J., Simonet, W. S., and Lacey, D. L. (2003) Osteoclast differentiation and activation. *Nature* **423,** 337–342
3. Komori, T., Yagi, H., Nomura, S., Yamaguchi, A., Sasaki, K., Deguchi, K., Shimizu, Y., Bronson, R. T., Gao, Y. H., Inada, M., Sato, M., Okamoto, R., Kitamura, Y., Yoshiki, S., and Kishimoto, T. (1997) Targeted disruption of Cbfa1 results in a complete lack of bone formation owing to maturational arrest of osteoblasts. *Cell* **89,** 755–764
4. Mundlos, S., Otto, F., Mundlos, C., Mulliken, J. B., Aylsworth, A. S., Albright, S., Lindhout, D., Cole, W. G., Henn, W., Knoll, J. H., Owen, M. J., Mertelsmann, R., Zabel, B. U., and Olsen, B. R. (1997) Mutations involving the transcription factor CBFA1 cause cleidocranial dysplasia. *Cell* **89,** 773–779
5. Otto, F., Thornell, A. P., Crompton, T., Denzel, A., Gilmour, K. C., Rosewell, I. R., Stamp, G. W., Beddington, R. S., Mundlos, S., Olsen, B. R., Selby, P. B., and Owen, M. J. (1997) Cbfa1, a candidate gene for cleidocranial dysplasia syndrome, is essential for osteoblast differentiation and bone development. *Cell* **89,** 765–771
6. Gong, Y., Slee, R. B., Fukai, N., Rawadi, G., Roman-Roman, S., Reginato, A. M., Wang, H., Cundy, T., Glorieux, F. H., Lev, D., Zacharin, M., Oexle, K., Marcelino, J., Suwairi, W., Heeger, S., Sabatakos, G., Apte, S., Adkins, W. N., Allgrove, J., Arslan-Kirchner, M., Batch, J. A., Beighton, P., Black, G. C., Boles, R. G., Boon, L. M., Borrone, C., Brunner, H. G., Carle, G. F., Dallapiccola, B., De Paepe, A., Floege, B., Halfhide, M. L., Hall, B., Hennekam, R. C., Hirose, T., Jans, A., Jüppner, H., Kim, C. A., Keppler-Noreuil, K., Kohlschuetter, A., LaCombe, D., Lambert, M., Lemyre, E., Letteboer, T., Peltonen, L., Ramesar, R. S., Romanengo, M., Somer, H., Steichen-Gersdorf, E., Steinmann, B., Sullivan, B., Superti-Furga, A., Swoboda, W., van den Boogaard, M. J., Van Hul, W., Vikkula, M., Votruba, M., Zabel, B., Garcia, T., Baron, R., Olsen, B. R., and Warman, M. L. (2001) LDL receptor-related protein 5 (LRP5) affects bone accrual and eye development. *Cell* **107,** 513–523
7. Brunkow, M. E., Gardner, J. C., Van Ness, J., Paeper, B. W., Kovacevich, B. R., Proll, S., Skonier, J. E., Zhao, L., Sabo, P. J., Fu, Y., Alisch, R. S., Gillett, L., Colbert, T., Tacconi, P., Galas, D., Hamersma, H., Beighton, P., and Mulligan, J. (2001) Bone dysplasia sclerosteosis results from loss of the SOST gene product, a novel cystine knot-containing protein. *Am. J. Hum. Genet.* **68,** 577–589
8. Kato, M., Patel, M. S., Levasseur, R., Lobov, I., Chang, B. H., Glass, D. A., 2nd, Hartmann, C., Li, L., Hwang, T. H., Brayton, C. F., Lang, R. A., Karsenty, G., and Chan, L. (2002) Cbfa1-independent decrease in osteoblast proliferation, osteopenia, and persistent embryonic eye vascularization in mice deficient in Lrp5, a Wnt coreceptor. *J. Cell Biol.* **157,** 303–314
9. Li, X., Ominsky, M. S., Niu, Q. T., Sun, N., Daugherty, B., D'Agostin, D., Kurahara, C., Gao, Y., Cao, J., Gong, J., Asuncion, F., Barrero, M., Warmington, K., Dwyer, D., Stolina, M., Morony, S., Sarosi, I., Kostenuik, P. J., Lacey, D. L., Simonet, W. S., Ke, H. Z., and Paszty, C. (2008) Targeted deletion of the sclerostin gene in mice results in increased bone formation and bone strength. *J. Bone Miner. Res.* **23,** 860–869
10. Jones, D. C., Wein, M. N., Oukka, M., Hofstaetter, J. G., Glimcher, M. J., and Glimcher, L. H. (2006) Regulation of adult bone mass by the zinc finger adapter protein Schnurri-3. *Science* **312,** 1223–1227
11. Wu, L. C. (2002) ZAS: C2H2 zinc finger proteins involved in growth and development. *Gene Expr.* **10,** 137–152
12. Jin, W., Takagi, T., Kanesashi, S. N., Kurahashi, T., Nomura, T., Harada, J., and Ishii, S. (2006) Schnurri-2 controls BMP-dependent adipogenesis via interaction with Smad proteins. *Dev. Cell* **10,** 461–471
13. Shim, J. H., Greenblatt, M. B., Zou, W., Huang, Z., Wein, M. N., Brady, N., Hu, D., Charron, J., Brodkin, H. R., Petsko, G. A., Zaller, D., Zhai, B., Gygi, S., Glimcher, L. H., and Jones, D. C. (2013) Schnurri-3 regulates ERK downstream of WNT signaling in osteoblasts. *J. Clin. Invest.* **123,** 4010–4022
14. Wein, M. N., Jones, D. C., Shim, J. H., Aliprantis, A. O., Sulyanto, R., Lazarevic, V., Poliachik, S. L., Gross, T. S., and Glimcher, L. H. (2012) Control of bone resorption in mice by Schnurri-3. *Proc. Natl. Acad. Sci. U.S.A.* **109,** 8173–8178
15. Liu, S., Madiai, F., Hackshaw, K. V., Allen, C. E., Carl, J., Huschart, E., Karanfilov, C., Litsky, A., Hickey, C. J., Marcucci, G., Huja, S., Agarwal, S., Yu, J., Caligiuri, M. A., and Wu, L. C. (2011) The large zinc finger protein ZAS3 is a critical modulator of osteoclastogenesis. *PloS One* **6,** e17161
16. Saita, Y., Takagi, T., Kitahara, K., Usui, M., Miyazono, K., Ezura, Y., Na-

kashima, K., Kurosawa, H., Ishii, S., and Noda, M. (2007) Lack of Schnurri-2 expression associates with reduced bone remodeling and osteopenia. *J. Biol. Chem.* **282,** 12907–12915
17. Jones, D. C., Schweitzer, M. N., Wein, M., Sigrist, K., Takagi, T., Ishii, S., and Glimcher, L. H. (2010) Uncoupling of growth plate maturation and bone formation in mice lacking both Schnurri-2 and Schnurri-3. *Proc. Natl. Acad. Sci. U.S.A.* **107,** 8254–8258
18. Saito, A., Hino, S., Murakami, T., Kanemoto, S., Kondo, S., Saitoh, M., Nishimura, R., Yoneda, T., Furuichi, T., Ikegawa, S., Ikawa, M., Okabe, M., and Imaizumi, K. (2009) Regulation of endoplasmic reticulum stress response by a BBF2H7-mediated Sec23a pathway is essential for chondrogenesis. *Nat. Cell Biol.* **11,** 1197–1204
19. Bobick, B. E., and Kulyk, W. M. (2004) The MEK-ERK signaling pathway is a negative regulator of cartilage-specific gene expression in embryonic limb mesenchyme. *J. Biol. Chem.* **279,** 4588–4595
20. Tominaga, H., Maeda, S., Hayashi, M., Takeda, S., Akira, S., Komiya, S., Nakamura, T., Akiyama, H., and Imamura, T. (2008) CCAAT/enhancer-binding protein β promotes osteoblast differentiation by enhancing Runx2 activity with ATF4. *Mol. Biol. Cell* **19,** 5373–5386
21. Alvarez, J., Sohn, P., Zeng, X., Doetschman, T., Robbins, D. J., and Serra, R. (2002) TGFβ2 mediates the effects of hedgehog on hypertrophic differentiation and PTHrP expression. *Development* **129,** 1913–1924
22. Ducy, P., Starbuck, M., Priemel, M., Shen, J., Pinero, G., Geoffroy, V., Amling, M., and Karsenty, G. (1999) A Cbfa1-dependent genetic pathway controls bone formation beyond embryonic development. *Genes Dev.* **13,** 1025–1036
23. Geoffroy, V., Kneissel, M., Fournier, B., Boyde, A., and Matthias, P. (2002) High bone resorption in adult aging transgenic mice overexpressing cbfa1/runx2 in cells of the osteoblastic lineage. *Mol. Cell. Biol.* **22,** 6222–6233
24. Kelleher, D. J., and Gilmore, R. (2006) An evolving view of the eukaryotic oligosaccharyltransferase. *Glycobiology* **16,** 47R–62R
25. Thiel, C., Schwarz, M., Peng, J., Grzmil, M., Hasilik, M., Braulke, T., Kohlschütter, A., von Figura, K., Lehle, L., and Körner, C. (2003) A new type of congenital disorders of glycosylation (CDG-Ii) provides new insights into the early steps of dolichol-linked oligosaccharide biosynthesis. *J. Biol. Chem.* **278,** 22498–22505
26. Moremen, K. W., and Molinari, M. (2006) *N*-Linked glycan recognition and processing: The molecular basis of endoplasmic reticulum quality control. *Curr. Opin. Struct. Biol.* **16,** 592–599
27. Aebi, M., Bernasconi, R., Clerc, S., and Molinari, M. (2010) *N*-Glycan structures: Recognition and processing in the ER. *Trends Biochem. Sci.* **35,** 74–82
28. Yang, X., Matsuda, K., Bialek, P., Jacquot, S., Masuoka, H. C., Schinke, T., Li, L., Brancorsini, S., Sassone-Corsi, P., Townes, T. M., Hanauer, A., and Karsenty, G. (2004) ATF4 is a substrate of RSK2 and an essential regulator of osteoblast biology; implication for Coffin-Lowry syndrome. *Cell* **117,** 387–398
29. Murakami, T., Saito, A., Hino, S., Kondo, S., Kanemoto, S., Chihara, K., Sekiya, H., Tsumagari, K., Ochiai, K., Yoshinaga, K., Saitoh, M., Nishimura, R., Yoneda, T., Kou, I., Furuichi, T., Ikegawa, S., Ikawa, M., Okabe, M., Wanaka, A., and Imaizumi, K. (2009) Signalling mediated by the endoplasmic reticulum stress transducer OASIS is involved in bone formation. *Nat. Cell Biol.* **11,** 1205–1211
30. Saito, A., Ochiai, K., Kondo, S., Tsumagari, K., Murakami, T., Cavener, D. R., and Imaizumi, K. (2011) Endoplasmic reticulum stress response mediated by the PERK-eIF2α-ATF4 pathway is involved in osteoblast differentiation induced by BMP2. *J. Biol. Chem.* **286,** 4809–4818
31. Korchynskyi, O., and ten Dijke, P. (2002) Identification and functional characterization of distinct critically important bone morphogenetic protein-specific response elements in the Id1 promoter. *J. Biol. Chem.* **277,** 4883–4891
32. Ishida, W., Hamamoto, T., Kusanagi, K., Yagi, K., Kawabata, M., Takehara, K., Sampath, T. K., Kato, M., and Miyazono, K. (2000) Smad6 is a Smad1/5-induced Smad inhibitor. Characterization of bone morphogenetic protein-responsive element in the mouse Smad6 promoter. *J. Biol. Chem.* **275,** 6075–6079
33. Garg, V., Muth, A. N., Ransom, J. F., Schluterman, M. K., Barnes, R., King, I. N., Grossfeld, P. D., and Srivastava, D. (2005) Mutations in NOTCH1 cause aortic valve disease. *Nature* **437,** 270–274
34. McLarren, K. W., Lo, R., Grbavec, D., Thirunavukkarasu, K., Karsenty, G., and Stifani, S. (2000) The mammalian basic helix loop helix protein HES-1 binds to and modulates the transactivating function of the runt-related factor Cbfa1. *J. Biol. Chem.* **275,** 530–538
35. Lee, J. S., Thomas, D. M., Gutierrez, G., Carty, S. A., Yanagawa, S., and Hinds, P. W. (2006) HES1 cooperates with pRb to activate RUNX2-dependent transcription. *J. Bone Miner. Res.* **21,** 921–933
36. Zaidi, S. K., Javed, A., Choi, J. Y., van Wijnen, A. J., Stein, J. L., Lian, J. B., and Stein, G. S. (2001) A specific targeting signal directs Runx2/Cbfa1 to subnuclear domains and contributes to transactivation of the osteocalcin gene. *J. Cell Sci.* **114,** 3093–3102
37. Kawamura, I., Maeda, S., Imamura, K., Setoguchi, T., Yokouchi, M., Ishidou, Y., and Komiya, S. (2012) SnoN suppresses maturation of chondrocytes by mediating signal cross-talk between transforming growth factor-β and bone morphogenetic protein pathways. *J. Biol. Chem.* **287,** 29101–29113
38. Dai, H., Hogan, C., Gopalakrishnan, B., Torres-Vazquez, J., Nguyen, M., Park, S., Raftery, L. A., Warrior, R., and Arora, K. (2000) The zinc finger protein schnurri acts as a Smad partner in mediating the transcriptional response to decapentaplegic. *Dev. Biol.* **227,** 373–387
39. Udagawa, Y., Hanai, J., Tada, K., Grieder, N. C., Momoeda, M., Taketani, Y., Affolter, M., Kawabata, M., and Miyazono, K. (2000) Schnurri interacts with Mad in a Dpp-dependent manner. *Genes Cells* **5,** 359–369
40. Zheng, Q., Zhou, G., Morello, R., Chen, Y., Garcia-Rojas, X., and Lee, B. (2003) Type X collagen gene regulation by Runx2 contributes directly to its hypertrophic chondrocyte-specific expression *in vivo*. *J. Cell Biol.* **162,** 833–842
41. Haeuptle, M. A., and Hennet, T. (2009) Congenital disorders of glycosylation: an update on defects affecting the biosynthesis of dolichol-linked oligosaccharides. *Hum. Mutat.* **30,** 1628–1641
42. Coman, D., Irving, M., Kannu, P., Jaeken, J., and Savarirayan, R. (2008) The skeletal manifestations of the congenital disorders of glycosylation. *Clin. Genet.* **73,** 507–515
43. Asada, R., Kanemoto, S., Kondo, S., Saito, A., and Imaizumi, K. (2011) The signalling from endoplasmic reticulum-resident bZIP transcription factors involved in diverse cellular physiology. *J. Biochem.* **149,** 507–518